Article (refereed) - postprint

Grünhage, Ludger; Pleijel, Håkan; Mills, Gina; Bender, Jürgen; Danielsson, Helena; Lehmann, Yvonne; Castell, Jean-Francois; Bethenod, Olivier. 2012 Updated stomatal flux and flux-effect models for wheat for quantifying effects of ozone on grain yield, grain mass and protein yield. *Environmental Pollution*, 165. 147-157. 10.1016/j.envpol.2012.02.026

Updated stomatal flux and flux-effect models for wheat for quantifying effects of ozone on grain yield, grain mass and protein yield

Ludger Grünhage [a,*], Håkan Pleijel [b], Gina Mills [c], Jürgen Bender [d], Helena Danielsson [e], Yvonne Lehmann [a], Jean-Francois Castell [f], Olivier Bethenod [g]

[a] Department of Plant Ecology, Justus-Liebig University, Heinrich-Buff-Ring 26, D-35392 Giessen, Germany
[b] Department of Plant and Environmental Sciences, University of Gothenburg, P.O. Box 461, SE-405 30 Gothenburg, Sweden
[c] Centre for Ecology and Hydrology, Environment Centre Wales, Deiniol Road, Bangor, UK, LL57 2UW
[d] Institute of Biodiversity, Johann Heinrich von Thünen-Institute (vTI), Federal Research Institute for Rural Areas, Forestry and Fisheries, Bundesallee 50, D-38116 Braunschweig, Germany
[e] IVL Swedish Environmental Research Institute Ltd., P.O. Box 5302, SE-400 14 Gothenburg, Sweden
[f] AgroParisTech, UMR 1091 EGC, F-78850 Thiverval-Grignon, France
[g] INRA, UMR 1091 EGC, F-78850 Thiverval-Grignon, France

_____

* Corresponding author:
Ludger Grünhage
Department of Plant Ecology, Justus-Liebig University, Heinrich-Buff-Ring 26, D-35392 Giessen, Germany
Tel.: +49 641 99 35314; fax: +49 641 99 19907.
E-mail address: Ludger.Gruenhage@bot2.bio.uni-giessen.de

ABSTRACT

Field measurements and open-top chamber experiments using nine current European winter wheat cultivars provided a data set that was used to revise and improve the parameterisation of a stomatal conductance model for wheat, including a revised value for maximum stomatal conductance and new functions for phenology and soil moisture. For the calculation of stomatal conductance for ozone a diffusivity ratio between O_3 and H_2O in air of 0.663 was applied, based on a critical review of the literature. By applying the improved parameterisation for stomatal conductance, new flux-effect relationships for grain yield, grain mass and protein yield were developed for use in ozone risk assessments including effects on food security. An example of application of the flux model at the local scale in Germany shows that negative effects of ozone on wheat grain yield were likely each year and on protein yield in most years since the mid 1980s.

Keywords: Ozone, diffusivity ratio, stomatal flux, flux-effect models, wheat, food security

Capsule

Improved parameterizations of ozone stomatal conductance model for wheat and new ozone flux-effect relationships for risk assessments.

1. Introduction

Tropospheric ozone (O_3) is regarded as the most important gaseous air pollutant affecting vegetation. During the last 100-150 years, the background O_3 concentration has increased by a factor up to five and is predicted to continue to increase (e.g. Marenco et al., 1994; Lelieveld and Dentener, 2000; Vingarzan, 2004). Since the mid 1980s, ground-level O_3 and its impact on human health and vegetation have increasingly come into focus within the LRTAP Convention[1] of the UNECE[2] and the European Union (EU). There is evidence of widespread adverse effects of O_3 on crops and (semi-)natural vegetation in Europe (Hayes et al., 2007; Mills et al., 2011a). As for all gaseous pollutants, the risk assessment methods for ozone to estimate effects on vegetation used by the LRTAP Convention are based on the exceedance of critical levels (CLs), defined as "the concentration, cumulative exposure or cumulative stomatal flux of atmospheric pollutants above which direct adverse effects on sensitive vegetation may occur according to present knowledge" (LRTAP Convention, 2010).

In the 1990s, exposure-response functions, mainly derived from experimental work in open-top chambers, were used to determine concentration-based CLs for ozone in Europe (based on AOT40[3]). However, one of the basic rules of toxicology is that dose-response relationships can only be established if the effective dose (flux) at the target site (e.g. membranes) or at least the absorbed dose (flux) of the stressor is known (Dämmgen et al., 1993; Grünhage and Jäger, 1996; Dämmgen and Grünhage, 1998; Musselman and Massman, 1999; Massman et al., 2000). Research over the last 10 years has led to significant developments in the methods for estimation of O_3 uptake by plants, modelled as the flux of O_3 from the atmosphere through the stomata (F_{st}; [nmol·m^{-2}·s^{-1}]). It has been shown that the cumulative O_3 uptake (POD_Y, Phytotoxic Ozone Dose; [mmol·m^{-2} PLA]) above a constant threshold flux of Y nmol m^{-2} PLA s^{-1} (PLA, projected leaf area, i.e. one-sided leaf area index) accumulated over a stated time period during daylight hours (global radiation > 50 W·m^{-2}),

$$POD_Y = \sum_{i=1}^{n} \left[\max\left(F_{st} - Y, 0\right) \cdot \Delta t\right]_i \quad (1)$$

provides stronger relationships with effects than external exposure indices such as AOT40 (Pleijel et al., 2004) and that flux-based risk maps provide a better fit to effects found in the field than AOT40-based risk maps (Mills et al. 2011a). POD_Y is calculated from hourly values of F_{st} so n denotes the number of hours included in the calculation and Δt = 1h. On the basis of these and other results, the LRTAP Convention has recommended that flux-based methods are considered for use in

[1] Convention on Long-Range Transboundary Air Pollution
[2] United Nations Economic Commission for Europe
[3] Accumulated ozone exposure over a threshold of 40 ppb, calculated from the hourly mean ozone concentrations at canopy height during daylight hours.

the revision of the Convention's Gothenburg Protocol to protect against effects of acidification, eutrophication and ground level ozone (Executive Body of LRTAP, 2009).

Recent progress in the development of a toxicologically appropriate dose metric to protect sensitive vegetation (crops, forest trees, (semi-)natural vegetation) was reviewed at LRTAP Convention workshops held in Ispra, Italy (2009) and as part of the 23rd ICP Vegetation[4] Task Force Meeting in Tervuren, Belgium (2010). At the latter meeting cumulative stomatal flux-based CLs were revised or derived for ten indicators, including effects on the yield of wheat, potato and tomato (LRTAP Convention, 2010 [updated Modelling and Mapping Manual], with critical level values also included in Mills et al., 2011b). For wheat, the revised/new CLs are based on the stomatal uptake by the flag leaf, which provides "an estimate of the critical amount of ozone entering through the stomata and reaching the sites of action inside the plant" (LRTAP Convention, 2010). The statistically derived constant flux threshold Y is interpreted as a provisional estimate of a detoxification threshold, below which it is assumed that O_3 molecules absorbed by the plant will be detoxified in the apoplast before reaching a target site (e.g. membranes).

The stomatal flux algorithm for wheat is based on the assumption that the O_3 concentration at the top of the canopy ($c_{O3}(z_h)$; [nmol·m^{-3}]) provides a reasonable estimate of the O_3 concentration at the upper surface boundary of the laminar boundary layer near the flag leaf, if the roughness sub-layer near the canopy is not taken into account (LRTAP Convention, 2010):

$$F_{st} = c_{O3}(z_h) \cdot g_{sto} \cdot \frac{1/(g_{sto} + g_{ext})}{R_b + 1/(g_{sto} + g_{ext})} \quad (2)$$

where g_{sto} represents the actual O_3 stomatal conductance of, in this case, the flag leaf of wheat [m·s^{-1}], g_{ext} the conductance of the external leaf surface for O_3 [m·s^{-1}] and R_b the resistance of the flag leaf laminar layer for O_3 [s·m^{-1}]. There is evidence from flux measurements that deposition of O_3 on e.g. external leaf surfaces exhibits diurnal variation (e.g. Gerosa et al., 2004). While work on models for non-stomatal O_3 deposition is in progress, g_{ext} has been provisionally set constant to 0.0004 m·s^{-1}.

The resistance of the flag leaf laminar layer for O_3 is given by:

$$R_b = 1.3 \cdot 150 \cdot \sqrt{\frac{L_{leaf}}{u(z_h)}} \quad (3)$$

with L_{leaf} the characteristic crosswind leaf dimension (in the case of the flag leaf 0.02 m) and $u(z_h)$ the horizontal wind velocity at canopy height [m·s^{-1}]. The constant 150 has the dimension s$^{0.5}$·m^{-1}, while the factor 1.3 accounts for the differences in diffusivity between sensible heat and ozone (Massman, 1998, 1999).

[4] International Cooperative Programme on Effects of Air Pollution on Natural Vegetation and Crops, reporting to the LRTAP Convention.

The dependency of the flag leaf stomatal conductance on solar radiation, temperature and water budgets of the atmosphere and soil as well as on the influence of phenology and O_3 is described according to a multiplicative Jarvis-Stewart approach (Jarvis, 1976; Stewart, 1988; Emberson et al., 2000a,b, Pleijel et al., 2007):

$$g_{sto} = g_{max} \cdot [\min(f_{phen}, f_{O3})] \cdot f_{light} \cdot \max\{f_{min}, (f_{temp} \cdot f_{VPD} \cdot f_{PAW})\} \quad (4)$$

where g_{max} represents the maximum value of the flag leaf stomatal conductance for ozone and the weighting factors f_x take values between 0 and 1 as a proportion of g_{max} (relative g). The g_{max} value described in Pleijel et al., (2007) was based on published data for six spring wheat cultivars (Kolibri, Astral, Boulmiche, Cadensa, Turbo and Dragon) and one durum wheat cultivar (Janus).

Even though it was generally accepted that the flux approach provided a better indicator of risk than the exposure-based CLs, the flux approach in its previous form (Pleijel et al., 2007) had a number of uncertainties. One uncertainty was associated with the fact that the dose-response relationship as well as the maximum value of stomatal conductance were derived from measurements performed in the past on wheat cultivars, most of which are currently not in use in agricultural practice: The cultivars Drabant and Satu (used in the dose-response relationship) as well as Kolibri, Boulmiche, Cadensa, Turbo and Janus (used in the derivation of g_{max}) have not been registered in the EU common catalogue of varieties (EU, 2009) for at least the last five years. Additionally, the relationships were based on spring wheat and durum wheat data, whilst in many parts of Europe winter wheat is the commercially-dominant cereal crop. Other uncertainties in the use of the multiplicative model for regional risk assessments are related to the parameterisation of phenology and soil water potential.

Because g_{max} of ozone is related to that of water vapour or carbon dioxide by the ratio of the respective molecular diffusivities, the value of g_{max} depends on an appropriate estimate of the molecular diffusivities. Although no new data were available for improving and validating the wheat dose-response relationship, new data for improvement of the parameterisation of the stomatal flux approach for wheat described by Pleijel at al. (2007) were available from field measurements and open-top chamber experiments on nine winter wheat cultivars that are currently in use commercially.

In this paper we describe an update of the Pleijel et al. (2007) model by incorporation of (1) a revised derivation of maximum stomatal conductance for wheat including re-consideration of molecular diffusivity for O_3; (2) revised Jarvis-Stewart functions for soil moisture conditions and phenology, including re-consideration of the toxicologically relevant accumulation period for stomatal uptake; (3) a revised dose-response function for effects on yield quantity and new response functions for effects on yield quality (protein yield and grain mass); and (4) by providing examples of the application of the flux-effect relationships for wheat in risk evaluations on a local scale.

Thus, the paper describes the progress made in improving the stomatal uptake-effect methodology in order to improve the accuracy of estimates of the risk of ozone pollution effects on wheat yield quantity and quality.

2. Material and methods

2.1. Stomatal conductance measurements

To improve the derivation of a maximum stomatal conductance for wheat, data from four sites were used: open-top chamber experiments performed in 2006 at Braunschweig, Germany and in 2003 from Vårgårda, 60 km northeast of Göteborg, Sweden, and measurements made in 2009 on wheat growing near Giessen and Braunschweig, Germany, and Grignon, near Paris, France. The 2006 study in Braunschweig was for the winter wheat cultivars Astron and Pegassos (cf. Schrader et al., 2009), n = 1031, whilst that for Sweden was for the spring wheat cultivar Vinjett (Uddling and Pleijel, 2006), n=120. In the 2009 studies, stomatal conductance was measured on field grown winter wheat cultivars (Opus, Manager, Carenius and Limes (n = 446) in Linden near Giessen, Cubus (n = 254) in Braunschweig, and Soissons (n = 206) and Premio (n = 224) in Grignon. The measurements performed in 2009 in Linden and Braunschweig as well as in 2003 in Vårgårda were used for the revision of the Jarvis-Stewart function for phenology and of the toxicologically relevant accumulation period for stomatal uptake. The measurement performed in Grignon in 2009 on the cultivars Soissons and Premio were used for validation.

The following measurements devices were used: in 2006 in Braunschweig and Sweden a portable photosynthesis system (LI-6400, LI-COR, Lincoln, Nebraska USA), in 2009 in Linden/Giessen and Braunschweig a leaf porometer (SC-1, Decagon Devices, Pullman, Washington USA) and in France in 2009 a portable photosynthesis system (CIRAS-2, PP Systems International, Amesbury, Maryland USA). Instruments were calibrated according to manufacturer's instructions.

2.2. Molecular diffusivity for ozone

While in the scientific literature consistent values for the molecular diffusivity constant for water vapour in air have been published, a range of values have been used for O_3. Based on the review of Massman (1998), a literature survey was conducted to clarify the scientific basis for the different diffusivity ratios and to determine the most appropriate one for the ozone flux model (see Appendix A).

2.3. Yield response functions

The dose response functions for the effects of O_3 on grain yield, grain mass and protein yield were derived using data sets described by Pleijel et al. (2007) and Piikki et al. (2008). These data were from thirteen experiments performed during 1987 to 1999 with field-grown crops with five cultivars (spring wheat: Minaret, Dragon, Drabant, Satu; durum wheat: Duilio) exposed to different O_3 levels in open-top chambers in four countries (Belgium, Finland, Italy and Sweden).

The regression of yield with POD_6 (Phytotoxic Ozone Dose above a flux threshold of 6 nmol m^{-2} s^{-1} projected leaf area) was based on the approach described by Fuhrer (1994), i.e. for each data set yield was calculated for zero POD_6. Thus, zero POD_6 was always associated with no effect at the individual experiment level, and relative yield from different experiments became comparable on a common, relative scale.

2.4. Modelled versus measured stomatal conductances

A first validation experiment was performed at a winter wheat field in Braunschweig in 2009. Canopy stomatal conductances derived from measurements with a portable gas exchange chamber system (Burkart et al., 2007) were compared with modelled stomatal conductances at leaf level which were upscaled to canopy level applying an improved version of de Pury and Farquhar (1997) sun-shade model (Grünhage et al., 2011).

2.5. Local risk evaluation

A local risk evaluation was performed applying the SVAT model CRO_3PS (Grünhage et al., 2011) based on the *big-leaf* model PLATIN (PLant-ATmosphere INteraction; Grünhage and Haenel, 1997, 2008) incorporating the revised flux model described here. Risk assessments were conducted with O_3 and meteorological data from the Environmental Monitoring and Climate Impact Research Station Linden near Giessen (www.uni-giessen.de/cms/ukl-en) and using the O_3 data from the monitoring station Radebeul-Wahnsdorf provided by Saxon State Agency for Environment, Agriculture and Geology (LfULG) and the meteorological data of the nearby station Dresden-Klotzsche of the German Weather Service. The calculations were conducted in four steps: (1) upscaling the stomatal conductance of the flag leaf to canopy level, (2) modelling total O_3 flux and calculation of O_3 concentration at canopy top, (3) calculation of flag leaf stomatal uptake and Phytotoxic Ozone Dose POD_6, and (4) calculation of potential yield loss.

3. Results and discussion

3.1. Derivation of flag leaf maximum stomatal conductance

According to the stomatal flux approach briefly described in the introduction, stomatal uptake estimations depend on the maximum stomatal conductance value for O_3 which can not be measured directly. Generally, the stomatal conductance for O_3 is related to that of water vapour or carbon dioxide by the ratio of the respective molecular diffusivities D:

$$g_{sto,O3} = g_{sto,H2O} \cdot \frac{D_{O3}}{D_{H2O}} \quad \text{or} \quad g_{sto,O3} = g_{sto,CO2} \cdot \frac{D_{O3}}{D_{CO2}} \tag{5}$$

Because the diffusivity of O_3 in air has never been measured, it must be derived from the known diffusivity of another gas or its characteristic properties.

The diffusivity ratios published in the literature (Table B1, Appendix B) show a variation of approx. 10 % and are derived applying the model of Chen and Othmer (1962), the model of Gilliland (1934) or Graham's law of diffusion (cf. Mason and Kronstadt, 1967).

The mean maximum stomatal conductance for O_3 of 450 mmol m^{-2} PLA s^{-1} derived in Pleijel et al. (2007) from 7 studies published between 1989 and 2003 was based on a diffusivity ratio D_{O3}/D_{H2O} of 0.613, a value which was derived by applying Graham's law of diffusion. As stated by Massman (1998) in his review on molecular diffusivities of trace gases, the application of Graham's law of diffusion for deriving molecular diffusivities from measured ones in air "is in opposition to all theoretical results". Appendix A has been included since Massman's proposed values have been largely ignored by the O_3 flux-effect community. It explains that the Massman diffusivity values at standard temperature and pressure (273.15 K, 1013.25 hPa) are based on a sounder concept. Massman's recommended molecular diffusivity for water vapour of 0.2178 cm^2 s^{-1} agreed well with the value of 0.219 ± 0.004 cm^2 s^{-1} derived by an independent literature survey of Grünhage and Haenel (1997). Massman's recommended value for the molecular diffusivity of O_3 is 0.1444 cm^2 s^{-1}. Based on the findings described in Appendix A, the ratios $D_{H2O,\,air}/D_{O3,\,air} = 1.51$ and $D_{O3,\,air}/D_{H2O,\,air} = 0.663$ were selected. The change to a diffusivity ratio of 0.663 has implications for several scientific areas including: (1) the paramaterisation for total O_3 flux densities in soil-vegetation-atmosphere-transfer models needs to be adapted, (2) the ratio of stomatal and non-stomatal O_3 flux will change, and (3) dose-response functions have to be updated.

The results from measurements on 9 winter wheat cultivars currently in use commercially performed in Linden, Braunschweig and Grignon are summarized in Figure 1 and compared with values in Pleijel et al. (2007). All g_{max} values for O_3 are based on the diffusivity ratio $D_{O3,\,air}/D_{H2O,\,air}$ of 0.663. Overall, the variation in the range of g_{max} values is somewhat lower in the "modern" wheat cultivars, i.e. cultivars currently in use, compared to the "older" ones, i.e. cultivars no longer grown but used in the derivation of g_{max} by Pleijel et al. (2007). The average of all g_{max} values, which are summarized in Table B2 (Appendix B), is 497 mmol O_3 m^{-2} s^{-1} (median: 492 mmol O_3 m^{-2} s^{-1}). For modelling purposes, a mean value of 500 mmol O_3 m^{-2} s^{-1} is recommended.

Obviously, the value of g_{max} is the most important factor in stomatal uptake calculations (cf. eq. 4). As illustrated in Fig. 1 g_{max} can vary to some extent from one wheat cultivar to another. For the evaluation of potential yield losses, g_{max} for the derivation of the stomatal uptake-effect relationships, and the g_{max} used in any specific crop loss assessment, must be identical. While the improved risk assessment methodology presented in this paper produces more realistic crop loss estimations, these may differ from the actual economic losses due to O_3 for a specific cultivar and a specific site.

3.2. Update of the Jarvis-Stewart functions

The stomatal conductance measurements performed on "modern" winter wheat cultivars were in agreement with the parameterizations for f_{light} and f_{temp} described by Pleijel et al (2007) (data not shown) while the functions for phenology and soil moisture needed updating. As a consequence of changing the diffusivity ratio $D_{O3,\,air}/D_{H2O,\,air}$ from 0.613 to 0.663 the coefficients of the Jarvis-Stewart function for O_3 were adjusted. The revised parameterisations of the functions for phenology, soil moisture and ozone are described below; the derivation of the unchanged functions (f_{light}, f_{temp}) are described Pleijel et al. (2007).

3.2.1. Phenology and toxicologically relevant accumulation period

The influence of phenology on flag leaf stomatal conductance (f_{phen}) is parameterised based on temperature sums (LRTAP Convention, 2010). In Pleijel et al. (2007) it was assumed that g_{max} occurred at mid-anthesis and the function shape was defined via two basic values, the start (A_{start}) and the end (A_{end}) of the accumulation period (linear increase of relative *g* from 0.8 to 1 between A_{start} and day of mid-anthesis ($A_{mid\text{-}anthesis}$), and a linear decrease of relative *g* from 1 to 0.2 between the day of mid-anthesis and A_{end}. The basis of this parameterisation was stomatal conductance measurements performed in Östad, Sweden, in 1996 and 1999.

The stomatal conductance measurements performed on the nine "modern" winter wheat cultivars and one spring wheat cultivar are summarized in Figure 2. Obviously, a decline of relative *g* from mid-anthesis to A_{start} could not be verified by the new data. Additionally, a linear decrease of relative *g* after mid-anthesis as assumed in the previous version of the Mapping Manual (LRTAP Convention, 2009) does not fit the new data.

Based on these new data sets, the following revised f_{phen} parameterisation based on thermal time accumulation (base temperature 0°C) is proposed. A_{start} will be equal to 200 degree days before $A_{mid\text{-}anthesis}$ and A_{end} to 700 degree days after $A_{mid\text{-}anthesis}$. Accordingly, stomatal uptake is now accumulated over a time period of 900 degree days which is slightly shorter than the period of 970

degree days used by Pleijel et al. (2007). As described in LRTAP Convention (2010), in the absence of observations from phenological networks, the timing of mid-anthesis can be estimated using a temperature sum of 1075 °C days calculated from plant emergence for spring wheat and after 1 January for winter wheat. This value is supported by the observations in the 2009 experiment in Grignon: mid-anthesis occurred 1089 °C days after 1 January for the winter wheat cultivar Soissons and 1102 °C days for the cultivar Premio.

Start and end of the integration period are expressed via temperature sums before (f_{phen_e}) and after (f_{phen_i}) mid-anthesis ($A_{mid\text{-}anthesis}$; f_{phen_f}) with the denotation of f_{phen} taken from LRTAP Convention (2010) and illustrated in Figure 2. The parameters f_{phen_a} and f_{phen_b} denote fractions of g_{max} that g_{sto} takes at specific development stages after mid-anthesis defined by f_{phen_g} and f_{phen_h}, if all other modifying factors are unity. Thus, the parameterization of f_{phen} is given by:

when $(f_{phen\_f} - f_{phen\_e}) \leq tt \leq (f_{phen\_f} + f_{phen\_g})$

$$f_{phen} = 1 \tag{6a}$$

when $(f_{phen\_f} + f_{phen\_g}) < tt \leq (f_{phen\_f} + f_{phen\_h})$

$$f_{phen} = 1 - \left(\frac{f_{phen\_a}}{f_{phen\_h} - f_{phen\_g}} \right) (tt - f_{phen\_g}) \tag{6b}$$

when $(f_{phen\_f} + f_{phen\_h}) < tt \leq f_{phen\_i}$

$$f_{phen} = f_{phen\_b} - \left(\frac{f_{phen\_b}}{f_{phen\_i} - f_{phen\_h}} \right) (tt - f_{phen\_h}) \tag{6c}$$

where tt is the effective temperature sum in degree days using a base temperature of 0 °C. By boundary line analysis f_{phen_a} is 0.3, f_{phen_b} = 0.7. f_{phen_e} = 200, f_{phen_f} = 0, f_{phen_g} = 100, f_{phen_h} = 525 and f_{phen_i} = 700 °C days.

As illustrated in Fig. 2a, the form of the revised phenology function (boundary line) fits to the measured conductances. Conductance measurements performed in Grignon, France, in 2009 support the new f_{phen} parameterisation (Fig. 2b). However, in comparison with the phenology relationship vs. °C days in CERES-Wheat (Ritchie and Otter, 1983), the revised phenology function shows a slightly delayed progress in senescence.

3.2.2. Soil moisture

In the previous versions of LRTAP Convention (2010), a Jarvis-Stewart function describing the effect of soil moisture on stomatal aperture based on soil water potential was used. This function was derived from data published in the peer-reviewed literature. Field evidence suggested that this function did not adequately represent stomatal conductance during periods of drought if the mean

soil water potential of the rooted soil layer is used (data not presented), and alternative approaches were evaluated. A conceptual change from a function based on soil water potential to one based on available plant soil water content (*PAW*; range of soil water in the rooted zone between field capacity (*PAW* = 100%) and permanent wilting point (*PAW* = 0%)) was applied.

There is evidence from field studies (Burkart et al. 2004, Grünhage et al. 2010, 2011) that stomatal conductance responds to *PAW* below a threshold of 50%. For the revised parameterisation of stomatal response to soil moisture content of wheat, the function according to Sadras and Milroy (1996) was selected:

$$f_{\mathrm{PAW}} = 1 \quad \text{if} \quad PAW_{\mathrm{t}} \le PAW \le 100\,\%$$
$$f_{\mathrm{PAW}} = 1 + \frac{PAW - PAW_{\mathrm{t}}}{PAW_{\mathrm{t}}} \quad \text{if} \quad PAW < PAW_{\mathrm{t}} \qquad (7)$$

where *PAW* is the actual plant available water content of the rooted zone [%] and PAW_{t} is the threshold *PAW* of 50 % above which relative stomatal conductance is at maximum, i.e. unity. Because the threshold may be depend on soil type, for risk assessments at a specific field site it is recommended to adapt the PAW_{t} value for the specific soil conditions.

3.2.3. Ozone

Based on observations of the onset of early senescence due to O_3 (Gelang et al., 2000; Pleijel et al., 1997), Pleijel et al. (2002) and Danielsson et al. (2003) included a Jarvis-Stewart function (f_{O3}) in g_{sto} parameterisation to allow for the influence of O_3 on stomatal conductance. The application of the updated diffusivity ratio required an adjustment of the coefficients used in Pleijel et al. (2007). The recalculated O_3 function is

$$f_{\mathrm{O3}} = \left(1 + \left(\frac{POD_0}{14}\right)^8\right)^{-1} \qquad (8)$$

where POD_0 is the Phytotoxic Ozone Dose accumulated from A_{start} without any threshold.

3.3. Updated stomatal flux-based response functions for effects on grain yield, grain mass and protein yield

Based on the updated parameterisation of the flag leaf stomatal conductance model described here, the stomatal uptake-effect relationships for effects on wheat were revised and new ones were derived (Figure 3):

$$\text{relative grain yield} = 1.00 - 0.038 \cdot POD_6$$

$$\text{relative grain mass} = 1.00 - 0.033 \cdot POD_6$$

$$\text{relative protein yield} = 1.01 - 0.025 \cdot POD_6$$

with POD_6 in mmol·m^{-2} PLA (PLA is the projected leaf area). The strongest correlations between relative yield (grain yield, grain mass, protein yield) and stomatal flux of O_3 to the flag leaf accumulated in the toxicologically relevant period during daylight hours (*POD*, Phytotoxic Ozone Dose) were obtained using an O_3 flux threshold of 6 nmol O_3 m^{-2} PLA s^{-1} (Pleijel et al., 2007). In comparison with Pleijel et al., (2007), the slope of the regression for effects on grain yield declines because the new stomatal uptake parameterization allows for larger stomatal flux. Because the R^2 values are similar to the earlier ones (grain yield: 0.83 → 0.84, grain mass: 0.75 → 0.71, protein yield: 0.59 → 0.63) it can be concluded that the model system used is robust. The new flux-effect relationships for relative grain mass (often expressed as "1000-grain weight" in an agronomic context) and relative protein yield (Figure 3b and c) provide comprehensive quality-based functions, particularly relevant in a of food security context.

The response functions shown in Figure 3 were used to derive new flux-based critical levels, above which direct adverse effects may occur (see Mills et al., 2011b for further details). The relationships described in Figure 3 are suitable for quantifying impacts of O_3 and assessing economic losses.

3.4. Modelled versus measured stomatal conductances

As illustrated in Figure 4, stomatal conductances calculated according to the new parameterization and upscaled to canopy level fit with canopy stomatal conductances derived from measurements with a portable gas exchange chamber system (Burkart et al., 2007) performed at a winter wheat field in Braunschweig in 2009. The modelled stomatal conductances at leaf level were upscaled to canopy level applying an improved version of de Pury and Farquhar (1997) sun-shade model; for details see Grünhage et al. (2011). T_{min} was adjusted to 10 °C based on site-specific observations. The experiment in Braunschweig provides the first validation of the new stomatal conductance parameterization at field level.

3.5. Examples of the application of the revised flux-effect models at the local scale

According to the European Council Directive on ambient air quality and cleaner air for Europe (Council Directive 2008/50/EC) local risk assessments for ozone have to be based on the parameters routinely measured by the European air quality monitoring networks. Recently, a SVAT model named CRO_3PS was published (Grünhage et al., 2011) which provides a validated

methodology for a local risk evaluation for winter wheat based on the critical level concept described here.

A risk evaluation performed for the fields at the Environmental Monitoring and Climate Impact Research Station Linden, Germany, illustrates the potentially strong influence of soil moisture on stomatal O_3 uptake and potential grain yield losses by including and excluding the influence of soil moisture in the rooted zone (Fig. 5). Assuming no soil water limitation on stomatal behaviour, i.e. $f_{PAW} = 1$, annual POD_6 values are 2 to 5 times higher than the *critical level* of 1 mmol m^{-2}. Such an analysis can be interpreted as a worst-case assessment for potential yield losses due to O_3, which provides the maximum potential yield loss. Depending on soil moisture conditions, POD_6 can be significantly reduced. The differences between both cases can be interpreted as the range of potential yield loss due to O_3 at a given site for a particular growing season. The extent of this range is likely to vary with the climatic conditions of the site, more humid sites having a smaller range.

A worst-case O_3 risk evaluation ($f_{Paw} = 1$) over 37 years for relative grain and protein yield is provided in Figure 6 for the monitoring station Radebeul-Wahnsdorf of the air quality monitoring network in Saxony, Germany. This monitoring station exhibits the longest O_3 time series in Germany (since 1974; Fig. 7). The effect of soil moisture could not be considered for this site, because hourly precipitation data are not available.

Annual POD_6 values increased gradually until the mid 1990s reaching more or less constant values of 4 to 5 mmol m^{-2} (Fig. 6). From the mid 1980s onwards the critical level of 1 mmol m^{-2} for relative wheat grain yield was exceeded every year up to a factor of 5 and the critical levels of 2 mmol m^{-2} for grain mass and protein yield were exceeded up to a factor of 2.5. Relative grain yield losses between 15 and 20 % were estimated since 1995 (Fig. 6a); between 9 and 12 % were predicted for relative protein yield losses (Fig. 6b).

4. Conclusions

The improvement of the stomatal conductance model for wheat described in this paper is based on conductance measurements made on nine different European winter wheat cultivars currently in use commercially and on a literature survey regarding the appropriate value for the molecular diffusivity for O_3. As a result of the new parameterisations of $g_{sto,\,max}$, f_{phen} and f_{PAW}, the modelled stomatal conductances agree well with upscaled conductances from measurements on winter wheat in Braunschweig. The slope of the regression between relative grain yield and POD_6 to the flag leaf as described in Pleijel et al. (2007) changed slightly, with a small improvement in R^2 from 0.83 to 0.84. Based on the data set described in Piikki et al. (2008), additional flux-effect relationships for relative grain mass and relative protein yield were derived for the first time for use in risk

assessment. Although the stomatal conductance model has been improved using data from currently grown cultivars of wheat, no new data sets are currently available to validate the above mentioned flux-effect relationships. Thus, the dose-response relationships are based on open-top chamber experiments with spring and durum wheat cultivars grown in the late 1980s and 1990s (cf. Pleijel et al., 2007). New exposure experiments, specifically designed to derive and test flux-effect relationships using the most recent cultivars, are required. However, the sensitivity of the response functions to the changes in the calibration of the conductance model was small, which indicates that the current response functions are robust.

Further improvements would include parameterisation of the dynamics of the O_3 detoxification capacity of the plants. Currently, the statistically derived constant flux threshold of 6 nmol m^{-2} PLA s^{-1} is removed from the calculated hourly stomatal flux during the accumulation period to account for detoxification. Obviously, this constant threshold flux does not reflect any temporal variation (diurnal or through the growing season) of the plant defence capacity. Despite these limitations, the improvements and validation of the parameterisations described here have provided robust flux-response relationships using data derived from four European countries with contrasting climates that are applicable for quantifying the growing threat from air pollution to both yield quantity and quality.

Using the flux-effect relationship described here, significant potential economic losses have been predicted for a large area of Europe including central European countries such as Germany and France, Mediterranean countries such as Italy, and northern countries such as the UK, Denmark and southern areas of Sweden assuming no soil water limitation on stomatal behaviour (i.e. worst-case assessment; Mills and Harmens, 2011). The improvements described in this paper have thus provided a risk assessment method that has been updated for modern cultivars and can be applied at a range of scales from local to regional to assess the growing threat from ozone pollution to the security of food supplies.

Acknowledgements

We thank the Hessian Agency for the Environment and Geology and the German Weather Service for providing the ozone and phenological data, respectively, and Carina Trenkler and Sybille Faust for field work assistance. The work by Håkan Pleijel and Helena Danielsson was supported by the Swedish Environment Protection Agency. Gina Mills thanks Defra (contracts AQ0810, AQ0816 and AQ0601), the LRTAP Convention and NERC for financial support of the coordination of the

ICP Vegetation. The work by Jean-François Castell and Olivier Bethenod was supported by the French National Research Agency, ANR, Vulnoz project.

References

Burkart, S., Manderscheid, R., Weigel, H.-J., 2004. Interactive effects of elevated atmospheric CO_2 concentrations and plant available water content on canopy evapotranspiration and conductance of spring wheat. European Journal of Agronomy 21, 401-417.

Burkart, S., Manderscheid, R., Weigel, H.-J., 2007. Design and performance of a portable gas exchange chamber system for CO_2- and H_2O-flux measurements in crop canopies. Environmental and Experimental Botany 61, 25-34.

Chen, N.H., Othmer, D.F., 1962. New generalized equation for gas diffusion coefficient. Journal of Chemical and Engineering 7, 37-41.

Council Directive 2008/50/EC of the European Parliament and of the Council of 21 May 2008 on ambient air quality and cleaner air for Europe. Official Journal of the European Union L 152, 11/06/2008, p. 1-44.

Dämmgen, U., Grünhage, L., 1998. Response of a grassland ecosystem to air pollutants. V. A toxicological model for the assessment of dose-response relationships for air pollutants and ecosystems. Environmental Pollution 101, 375-380.

Dämmgen, U., Grünhage, L., Haenel, H.-D., Jäger, H.-J., 1993. Climate and stress in ecotoxicology. A coherent system of definitions and terms. Angewandte Botanik 67, 157-162.

Danielsson, H., Karlsson, G.P., Karlsson, P.E., Pleijel, H., 2003. Ozone uptake modelling and flux-response relationships - an assessment of ozone-induced yield loss in spring wheat. Atmospheric Environment 37, 475-485.

de Pury, D.G.G., Farquhar, G.D., 1997. Simple scaling of photosynthesis from leaves to canopies without the errors of big-leaf models. Plant, Cell and Environment 20, 537-557.

Emberson, L.D., Ashmore, M.R., Cambridge, H.M., Simpson, D., Tuovinen, J.-P., 2000a. Modelling stomatal ozone flux across Europe. Environmental Pollution 109, 403-413.

Emberson, L.D., Simpson, D., Tuovinen, J.-P., Ashmore, M.R., Cambridge, H.M., 2000b. Towards a model of ozone deposition and stomatal uptake. EMEP MSC-W Note 6/00. Oslo: Norwegian Meteorological Institute.

Erisman, J.W., van Pul, A., Wyers, P., 1994. Parameterization of surface resistance for the quantification of atmospheric deposition of acidifying pollutants and ozone. Atmospheric Environment 28, 2595-2607.

EU, 2009. Information from European Union Instructions and Bodies Commission. Common catalogue of Varieties of agricultural plant species. 28th complete edition. Official Journal of the European Union C 302 A/01, 1-639.

Executive Body for LRTAP, 2009. ECE.EB.AIR/96. Report of the Executive Body on its twenty-sixth session held in Geneva from 15 to 18 December 2008. (available at http://www.unece.org/env/lrtap/ExecutiveBody/welcome.26.html)

Fuhrer, J., 1994. The critical level for ozone to protect agricultural crops - an assessment of data from European open-top chamber experiments. In: Fuhrer, J., Achermann, B. (Eds.), Critical Levels for Ozone - a UN-ECE workshop report. FAC Schriftenreihe (Eidgenössische Forschungsanstalt für Agrikulturchemie und Umwelthygiene, Bern) Nr. 16, pp. 42-57.

Gelang, J., Pleijel, H., Sild, E., Danielsson, H., Younis, S., Selldén, G., 2000. Rate and duration of grain filling in relation to flag leaf senescence and grain yield in spring wheat (Triticum aestivum) exposed to different concentrations of ozone. Physiologia Plantarum 110, 366-375.

Gerosa, G., Marzuoli, R., Cieslik, S., Ballarin-Denti, A., 2004. Stomatal ozone fluxes over a barley field in Italy. "Effective exposure" as a possible link between exposure- and flux-based approaches. Atmospheric Environment 38, 2421-2432.

Gilliland, E.R., 1934. Diffusion coefficients in gaseous systems. Industrial and Engineering Chemistry 26, 681-685.

Grünhage, L., Braden, H., Bender, J., Burkart, S., Lehmann, Y., Schröder, M., 2011: Evaluation of the ozone-related risk for winter wheat at local scale with the CRO_3PS model. Gefahrstoffe - Reinhaltung der Luft 71, 90-97. (available at http://www.uni-giessen.de/cms/CRO3PS)

Grünhage, L., Haenel, H.-D., 1997. PLATIN (PLant-ATmosphere INteraction) I: a model of plant-atmosphere interaction for estimating absorbed doses of gaseous air pollutants. Environmental Pollution 98, 37-50.

Grünhage, L., Haenel, H.-D., 2008. Detailed documentation of the PLATIN (PLant-ATmosphere INteraction) model. Landbauforschung Völkenrode, special issue 319, 1-85. (available at http://www.uni-giessen.de/cms/ukl-en/PLATIN)

Grünhage, L., Jäger, H.-J., 1996. Critical levels for ozone, ozone exposure potentials of the atmosphere or critical absorbed doses for ozone: a general discussion. In: Kärenlampi, L., Skärby, L. (Eds.), Critical levels for ozone in Europe: testing and finalizing the concepts. UN-ECE workshop report. University of Kuopio, Department of Ecology and Environmental Science, Kuopio, pp. 151-168.

Grünhage, L., Lehmann, Y., Schröder, M., Braden, H., Bender, J., Burkart, S., Hanewald, K., 2010. CRO_3PS - an ozone risk evaluation model for winter wheat at local scale. In: Wuyts, K., Samson, R., de Maerschalck, B., Kardel, F., Janssen, S., Engelen, M. (Eds.): Proceedings of the international conference on Local Air Quality and its Interactions with Vegetation. January 21-22, 2010, Antwerp, Belgium. VITO & University of Antwerp, within the framework of the CLIMAQS project (IWT-SBO), Antwerp, pp. 43-48.

Hayes, F., Mills, G., Harmens, H., Norris, D., 2007. Evidence of widespread ozone damage to vegetation in Europe. Bangor, UK: ICP Vegetation Programme Coordination Centre, Centre for Ecology & Hydrology. (available at http://icpvegetation.ceh.ac.uk)

Hodgman, C.D., Weast, R.C., Selby, S.M., 1956. Handbook of chemistry and physics, ed. 37. Chemical Rubber Publ. Co., Cleveland, Ohio.

Jarvis, P.G., 1976. The interpretation of the variations in leaf water potential and stomatal conductance found in canopies in the field. Philosophical Transactions of the Royal Society of London Series B - Biological Sciences 273, 593-610.

Laisk, A., Kull, O., Moldau, H., 1989. Ozone concentration in leaf intercellular air spaces is close to zero. Plant Physiology 90, 1163-1167.

Lelieveld, J., Dentener, F.J., 2000. What controls tropospheric ozone? Journal of Geophysical Research - Atmosphere 105, 3531-3551.

Lide, D.R., 1992: CRC handbook of chemistry and physics, ed. 73. CRC Press, Boca Raton, Florida.

LRTAP Convention, 2009. Mapping Manual 2004. Manual on methodologies and criteria for modelling and mapping critical loads & levels and air pollution effects, risk and trends. Chapter 3. Mapping critical levels for vegetation. 2009 revision.

LRTAP Convention, 2010. Mapping Manual 2004. Manual on methodologies and criteria for modelling and mapping critical loads & levels and air pollution effects, risk and trends. Chapter 3. Mapping critical levels for vegetation. 2010 revision. (available at http://icpvegetation.ceh.ac.uk)

Marenco, A., Gouget, H., Nédélec, P., Pagés, J.-P., Karcher, F., 1994. Evidence of a long-term increase in tropospheric ozone from Pic du Midi data series: Consequences: Positive radiative forcing. Journal of Geophysical Research - Atmosphere 99, 16617-16632.

Mason, E.A., 1971. Diffusion in gases. In: Sherwood, J.N., Chadwick, A.V., Muir, W.M., Swinton, F.L. (Eds.): Diffusion processes. Proceedings of the Thomas Graham Memorial Symposium, University of Strathclyde, Vol. 1. Gordon and Breach, London, pp. 3-27.

Mason, E.A., Evans, R.B., 1969. Graham's Laws: Simple demonstrations of gases in motion. Journal of Chemical Education 46, 358-364.

Mason, E.A., Kronstadt, B., 1967. Graham's Laws of diffusion and effusion. Journal of Chemical Education 44, 740-744.

Massman, W.J., 1998. A review of the molecular diffusivities of H_2O, CO_2, CH_4, CO, O_3, SO_2, NH_3, N_2O, NO, and NO_2 in air, O_2 and N_2 near STP. Atmospheric Environment 32, 1111-1127.

Massman, W.J., 1999. Molecular diffusivities of Hg vapor in air, O_2 and N_2 near STP and the kinematic viscosity and thermal diffusivity of air near STP. Atmospheric Environment 33, 453-457.

Massman, W.J., Musselman, R.C., Lefohn, A.S., 2000. A conceptual ozone dose-response model to develop a standard to protect vegetation. Atmospheric Environment 34, 745-759.

Mills, G., Hayes, F., Simpson, D., Emberson, L., Norris, D., Harmens, H., Büker, P., 2011a. Evidence of widespread effects of ozone on crops and (semi-)natural vegetation in Europe (1990-2006) in relation to AOT40- and flux-based risk maps. Global Change Biology 17, 592-613.

Mills, G., Pleijel, H., Braun, S., Büker, P., Bermejo, V., Calvo, E., Danielsson, H., Emberson, L., González Fernández, I., Grünhage, L., Harmens, H., Hayes, F., Karlsson, P.-E., Simpson, D., 2011b. New stomatal flux-based critical levels for ozone effects on vegetation. Atmospheric Environment, 45, 5064 – 5068.

Mills, G., Harmens, H. (eds). 2011. Ozone pollution: A hidden threat to food security. Programme Coordination Centre for the ICP Vegetation, Centre for Ecology and Hydrology, Bangor, UK. ISBN 978-1-906698-27-0. (available at http://icpvegetation.ceh.ac.uk)

Musselman, R.C., Massman, W.J., 1999. Ozone flux to vegetation and its relationship to plant response and ambient air quality standards. Atmospheric Environment 33, 65-73.

Perry, J.H., 1950. Chemical engineers handbook. 3rd ed. New York: McGraw-Hill.

Piikki, K., De Temmerman, L., Ojanperä, K., Danielsson, H., Pleijel, H., 2008. The grain quality of spring wheat (*Triticum aestivum* L.) in relation to elevated ozone uptake and carbon dioxide exposure. European Journal of Agronomy 28, 245-254.

Pleijel, H., Danielsson, H., Emberson, L., Ashmore, M., Mills, G., 2007. Ozone risk assessment for agricultural crops in Europe: Further development of stomatal flux and flux-response relationships for European wheat and potato. Atmospheric Environment 41, 3022-3040.

Pleijel, H., Danielsson, H., Ojanperä, K., De Temmerman, L., Högy, P., Badiani, M., Karlsson, P.E., 2004. Relationships between ozone exposure and yield loss in European wheat and potato - a comparison of concentration- and flux-based exposure indices. Atmospheric Environment 38, 2259-2269.

Pleijel, H., Danielsson, H., Vandermeiren, K., Blum, C., Colls, J., Ojanperä, K., 2002. Stomatal conductance and ozone exposure in relation to potato tuber yield - results from the European CHIP programme. European Journal of Agronomy 17, 303-317.

Pleijel, H., Ojanperä, K., Danielsson, H., Sild, E., Gelang, J., Wallin, G., Skärby, L., Selldén, G., 1997. Effects of ozone on leaf senescence in spring wheat - possible consequences for grain yield. Phyton (Horn, Austria) 37, 227-232.

Ritchie, J.T., Otter, S., 1983. Description and performance of CERES-Wheat: A user-oriented wheat yield model. USDA-ARS, Grassland Soil and Water Laboratory, Temple, Texas.

Sadras, V.O., Milroy, S.P., 1996. Soil-water thresholds for the responses of leaf expansion and gas exchange: A review. Field Crops Research 47, 253-266.

Schrader, S., Bender, J., Weigel, H.J., 2009. Ozone exposure of field-grown winter wheat affects the diversity of soil mesofauna in the rhizosphere. Environmental Pollution 157, 3357-3362.

Simpson, D., Fagerli, H., Jonson, J.E., Tsyro, S., Wind, P., Tuovinen, J.-P., 2003. Transboundary acidification, eutrophication and ground level ozone in Europe. EMEP Status Report 1, Part I: Unified EMEP model description. Norwegian Meteorological Institute, Oslo.

Stewart, J.B., 1988. Modelling surface conductance of pine forest. Agricultural and Forest Meteorology 43, 19-35.

Uddling, J., Pleijel, H., 2006. Changes in stomatal conductance and net photosynthesis during phenological development in spring wheat: implications for gas exchange modelling. International Journal of Biometeorology 51, 37-48.

Vingarzan, R., 2004. A review of surface ozone background levels and trends. Atmospheric Environment 38, 3431-3442.

Weast, R.C., Astle, M.J., 1983. Handbook of chemistry and physics, ed. 63. CRC Press, Boca Raton, Florida.

Wesely, M.L., 1989. Parameterization of surface resistances to gaseous dry deposition in regional-scale numerical models. Atmospheric Environment 23, 1293-1304.

Wesely, M.L., Eastman, J.A., Stedman, D.H., Yalvac, E.D., 1982. An eddy-correlation measurement of NO_2 flux to vegetation and comparison to O_3 flux. Atmospheric Environment 16, 815-820.

Appendix A: Derivation of molecular diffusivity for O_3

As mentioned in section 4.1, the diffusivity ratios summarized in Table B1 (Appendix B) are derived applying three different concepts:

- the model of Chen and Othmer (1962),
- the model of Gilliland (1934)

or

- Graham's law of diffusion (cf. Mason and Kronstadt, 1967).

Laisk et al. (1989) and Massman (1998) calculated D_{O3} [$cm^2 \cdot s^{-1}$] applying the Chen-Othmer model:

$$D(T,p) = \frac{2.616 \cdot \sqrt{1/M_i + 1/M_j} \cdot \left(T/T_0\right)^{1.81}}{\left(\frac{Tc_i \cdot Tc_j}{10^4}\right)^{0.1405} \cdot \left[\left(\frac{Vc_i}{100}\right)^{0.4} + \left(\frac{Vc_j}{100}\right)^{0.4}\right]^2} \quad \text{(A1)}$$

where T is the temperature exposed in K and p the standard pressure of 1 atmosphere. The subscripts "i" and "j" refer to the specific gases under consideration, M_i and M_j are their respective molecular masses [g mol^{-1}], Tc_i and Tc_j are their respective critical temperature [K] and Vc_i and Vc_j are their respective critical volumes [cm^3 mol^{-1}]. The three characteristic parameters were extracted by Laisk et al. (1989) as well as by Massman (1998) from the "CRC Handbook of Chemistry and Physics", while Massman (1998) refer to edition no. 73 (Lide, 1992) and Laisk et al. (1989) to the older ones no. 37 (Hodgman et al., 1956) and no. 63 (Weast and Astle, 1983).

Massman (1998) calculates D_{O3} in O_2 and N_2. Applying Blanc's law yields for $D_{O3,\,air}$:

$$D_{O3,air}(T,p) = \left[\frac{0.79}{D_{O3,N2}(T,p)} + \frac{0.21}{D_{O3,O2}(T,p)}\right]^{-1} \quad \text{(A2)}$$

The ratio D_{H2O}/D_{O3} from Erisman et al. (1994) was derived applying the model of Gilliland (1934) and the values given in Perry (1950):

$$D = 0.0043 \cdot \frac{T^{3/2}}{p \cdot (V_i^{1/3} + V_j^{1/3})^2} \cdot \sqrt{\frac{1}{M_i} + \frac{1}{M_j}} \quad \text{(A3)}$$

with T is the temperature [K], p the atmospheric pressure [atm], the subscripts "i" and "j" refer to the specific gases under consideration, M_i and M_j are their respective molecular masses [g mol^{-1}] and V_i and V_j are their molecular volumes at the normal boiling points [cm^2/g.mole]. The ratio given in Erisman et al. (1994) results if gas i is O_3 and gas j is H_2O.

The other values given in Table B1 (Appendix B) are based on Graham's law of diffusion. It can be stated as follows: "*when two gases interdiffuse at uniform pressure, their fluxes are in the inverse*

ratio of the square roots of their molecular weights" (Mason and Kronstadt, 1967; Mason and Evans 1969; Mason 1971):

$$-\frac{J_i}{J_j} = \sqrt{\frac{M_j}{M_i}} \qquad \text{(A4)}$$

As cited in Mason and Kronstadt (1967), the assumption that "*the diffusion coefficients of gases 2* (identical to gas i in eqs. above) *and 3* (identical to gas j in eqs. above) *into a reference gas 1 should vary inversely as the square roots of the molecular weights of 2 and 3*",

$$-\frac{J_2}{J_3} = \frac{D_{12}}{D_{13}} \approx \sqrt{\frac{M_3}{M_2}} \qquad \text{(A5)}$$

is "*only a crude approximation for most systems, although it is correct in the limiting case that the reference gas 1 has molecules which are infinitely large and heavy compared to molecules of 2 and 3*". Obviously, this precondition is not met by air as reference gas 1 and is the explanation for the different values for $D_{O3,\,air}/D_{H2O,\,air}$ given in Table B1 (Appendix B).

Massman (1998) stated that "*the misapplication of Graham's law*" according to

$$\frac{D_{O3,air}}{D_{H2O,air}} = \frac{D_{x,air} \cdot \sqrt{\frac{M_x}{M_{O3}}}}{D_{H2O,air}} \qquad \text{(A6)}$$

"*is in opposition to all theoretical results*". The coincidence of the ratios of Massman (1998) and Grünhage and Haenel (1997, 2008) can be explained by the choice of O_2 as gas "x" and the applied value of D_{O2}.

Appendix B

Table B1
Diffusivity (D) ratios of different gases in air published in the literature. M is molar mass.

D_{H2O}/D_{O3}	D_{O3}/D_{H2O}	Publication
ACCORDING TO CHEN & OTHMER (1962), CF. APPENDIX A		
1.67	0.599	Laisk et al. (1989)
1.51	0.663	calculated according to diffusivities cited in Massman (1998)
ACCORDING TO GILLILAND (1934) AND PERRY (1950), CF. APPENDIX A		
1.5	0.667	Erisman et al. (1994)
ACCORDING TO GRAHAM'S LAW OF DIFFUSION (CF. MASON & KRONSTADT 1967), CF. APPENDIX A $D_{O3} = D_{H2O} \cdot \sqrt{(M_{H2O}/M_{O3})}$		
1.63	0.613	recalculated from values given in Pleijel et al. (2007)
1.6	0.625	Simpson et al. (2003) after Wesely (1989)
1.67	0.6	Emberson et al. (2000b)
1.64	0.61	Wesely et al. (1982)
1.6	0.625	Wesely (1989)
$D_{O3} = D_{O2} \cdot \sqrt{(M_{O2}/M_{O3})} = 0.145$ cm^2 s^{-1} with $D_{O2} = 0.178$ cm^2 s^{-1} and $D_{H2O} = 0.219 \pm 0.004 \cdot$cm^2 s^{-1}		
1.51	0.662	Grünhage & Haenel (1997)
$D_{O3} = D_{CO2} \cdot \sqrt{(M_{CO2}/M_{O3})} = 0.131$ cm^2 s^{-1} with $D_{CO2} = 0.137 \pm 0.004$ cm^2 s^{-1} and $D_{H2O} = 0.219 \pm 0.004 \cdot$cm^2 s^{-1}		
1.67	0.598	calculated from values given in Grünhage and Haenel (1997)

Table B2
Click here to download Table: Table B2.doc

Appendix B

Table B2

Derivation of mean flag leaf maximum stomatal conductance for ozone ($D_{O3,\,air}/D_{H2O,\,air}$ = 0.663)

Wheat type and cultivar	Country	Growing conditions	Measuring apparatus	Time of day	Time of year	g_{max} derivation	g_{max} [mmol O_3 m^{-2} s^{-1} PLA]
Spring wheat, Kolibri	Spain	Field	LI-COR 1600	9 to 13 hrs	14 March to 21 May	cf. LRTAP Convention (2009)	435
Spring wheat, Astral	Spain	Field	LI-COR 1600	9 to 13 hrs	14 March to 21 May	cf. LRTAP Convention (2009)	376
Spring wheat, Boulmiche	Spain	Field	LI-COR 1600	9 to 13 hrs	14 March to 21 May	cf. LRTAP Convention (2009)	366
Spring wheat, Cadensa	Denmark	Field Lysimeter	LI-COR 6200	(Assumed mid-day)	August	cf. LRTAP Convention (2009)	660
Spring wheat, Turbo	Germany	Field	LI-COR 1600	11 to 12 hrs	17 June to 7 August	cf. LRTAP Convention (2009)	525
Spring wheat, Dragon	Sweden	Field OTC & AA	LI-COR 6200	13 hrs	13 August 1996 (AA)	cf. LRTAP Convention (2009)	548
Durum wheat, Janus	Austria	Field	Ventilated diffusion porometer	-	-	cf. LRTAP Convention (2009)	492
Winter wheat, Astron	Germany	OTC (NF)	LI-COR 6400	measured at 10 hrs	24 May to 14 June 2006	653 mmol H_2O m^{-2} s^{-1}	433
Winter wheat, Pegassos	Germany	OTC (NF)	LI-COR 6400	measured at 10 CET	24 May to 14 June 2006	650 mmol H_2O m^{-2} s^{-1}	431
Winter wheat, Opus	Germany	Field	Decagon SC-1	measured at 11 CET	26 May to 02 June 2009	839 mmol H_2O m^{-2} s^{-1} (adaxial=524, abaxial=315)	556
Winter wheat, Manager - *)	Germany	Field	Decagon SC-1	measured at 10 CET	26 May to 02 June 2009	770 mmol H_2O m^{-2} s^{-1} (adaxial=439, abaxial=331)	511
Winter wheat, Carenius	Germany	Field	Decagon SC-1	measured at 13 CET	26 May to 02 June 2009	729 mmol H_2O m^{-2} s^{-1} (adaxial=451, abaxial=278)	483
Winter wheat, Manager + *)	Germany	Field	Decagon SC-1	measured at 11:30 CET	26 May to 02 June 2009	849 mmol H_2O m^{-2} s^{-1} (adaxial=485, abaxial=364)	563
Winter wheat, Limes	Germany	Field	Decagon SC-1	measured at 11:30 CET	26 May to 02 June 2009	766 mmol H_2O m^{-2} s^{-1} (adaxial=510, abaxial=256)	508
Winter wheat, Cubus	Germany	Field	Decagon SC-1	measured at 11:30 CET	20 May to 02 June 2009	894 mmol H_2O m^{-2} s^{-1} (adaxial=595, abaxial=299)	593
Winter wheat, Soissons	France	Field	PP systems CIRAS-2	11 to 16 CET	6 to 27 May 2009	714.4 ± 42.1 mmol H_2O m^{-2} s^{-1}	474
Winter wheat, Premio	France	Field	PP systems CIRAS-2	11 to 16 CET	6 to 27 May 2009	741.6 ± 72.8 mmol H_2O m^{-2} s^{-1}	492

*) Manager - : cultivar Manager grown at a field with non-optimal soil water conditions due to soil texture
Manager + : cultivar Manager grown at a field with optimal soil water conditions due to soil texture

Note: Data from LRTAP Convention (2009) can be found in Pleijel et al. (2007)

Figure captions:

Fig. 1. Maximum stomatal conductance for wheat ($D_{O3,\ air}/D_{H2O,\ air}$ = 0.663) in a range of different cultivars. (dots: g_{max} values described in the previous version of the LRTAP Convention's Mapping Manual; diamonds: g_{max} values derived from measurements on winter wheat cultivars currently in use commercially)

Fig. 2a. Relative stomatal conductance and boundary line for the modifying influence of phenology on stomatal conductance vs. thermal time from day of mid-anthesis.

Fig. 2b. Relative stomatal conductance and boundary line for the modifying influence of phenology on stomatal conductance vs. thermal time from day of mid-anthesis. Validation data set.

Fig. 3. The relationship between relative yield of wheat and Phytotoxic Ozone Dose above a threshold flux of 6 nmol m^{-2} s^{-1} (POD_6) for the flag leaf based on five wheat cultivars from three or four European countries (BE: Belgium, FI: Finland, IT: Italy, SE: Sweden) using effective temperature sum to describe phenology: a) relative grain yield, b) relative grain mass, and c) relative protein yield. The dashed lines indicate the 95%-confidence intervals.

Fig. 4. Modelled leaf level stomatal conductance upscaled to canopy level vs. measured canopy stomatal conductance. Comparison period: 2009-06-06 to 2009-06-17, 11 am to 4 pm CET.

Fig. 5. Phytotoxic Ozone Dose (POD_6) and potential grain yield loss for Linden, Hesse, Germany. Risk evaluation according to the LRTAP Convention's Mapping Manual (LRTAP Convention, 2010)

- "black and white" for the printed version
- "coloured" for the Web

Fig. 6a. Phytotoxic Ozone Dose (POD_6) and potential grain yield loss for Radebeul-Wahnsdorf, Saxony. Worst-case risk evaluation according to the LRTAP Convention's Mapping Manual (LRTAP Convention, 2010)
data source: O_3 concentration - air quality monitoring network Saxony, meteorological data - monitoring station Dresden-Klotzsche of the German Weather Service

- "black and white" for the printed version
- "coloured" for the Web

Fig. 6b. Phytotoxic Ozone Dose (POD_6) and potential protein yield loss for Radebeul-Wahnsdorf, Saxony. Worst-case risk evaluation according to the LRTAP Convention's Mapping Manual (LRTAP Convention, 2010)
data source: O_3 concentration - air quality monitoring network Saxony, meteorological data - monitoring station Dresden-Klotzsche of the German Weather Service

- "black and white" for the printed version
- "coloured" for the Web

Fig. 7. Time series of mean O_3 concentration at the air quality monitoring station Radebeul-Wahnsdorf, Germany

- "black and white" for the printed version
- "coloured" for the Web

Figure 1

Click here to download high resolution image

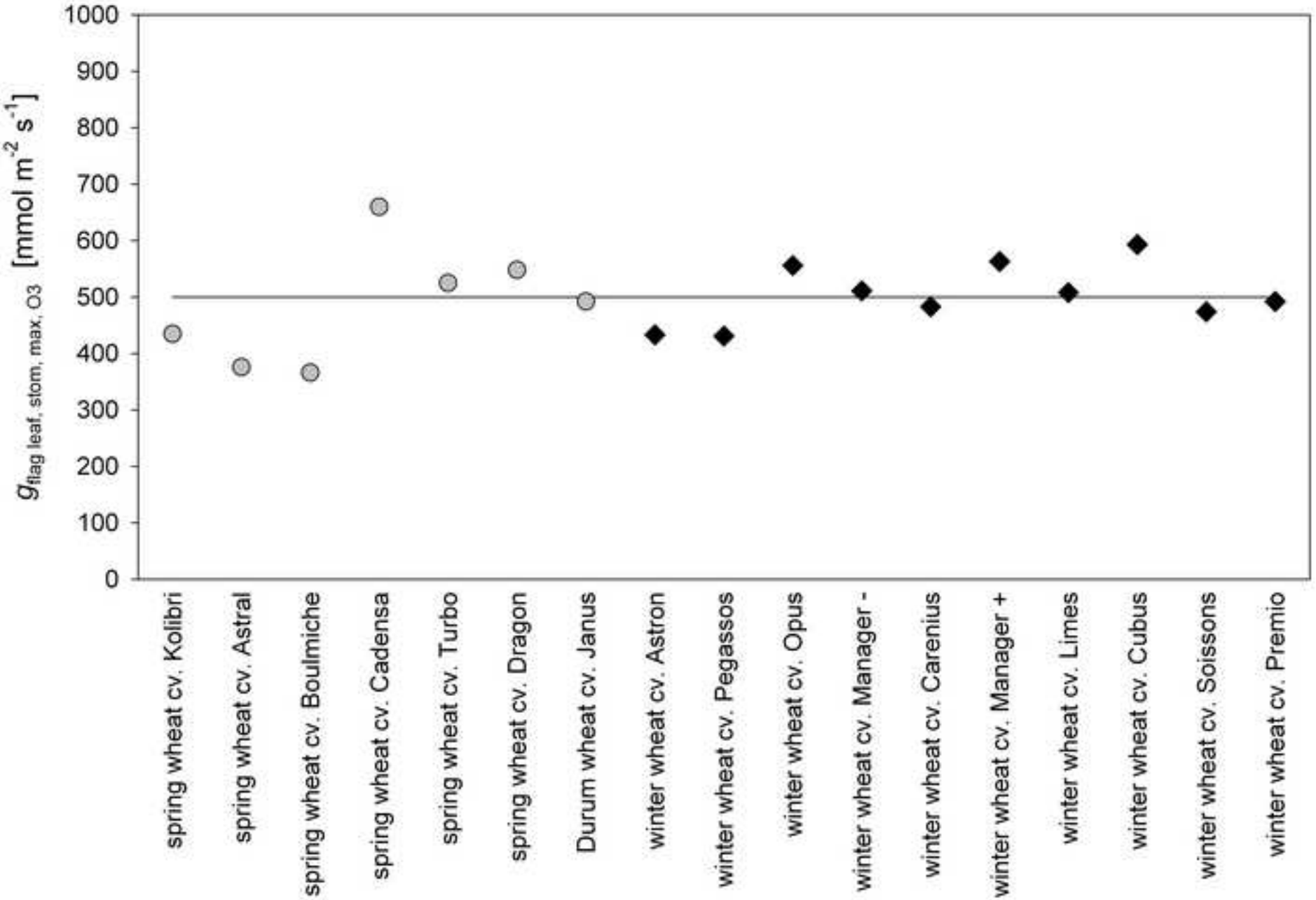

Figure 2a

Click here to download high resolution image

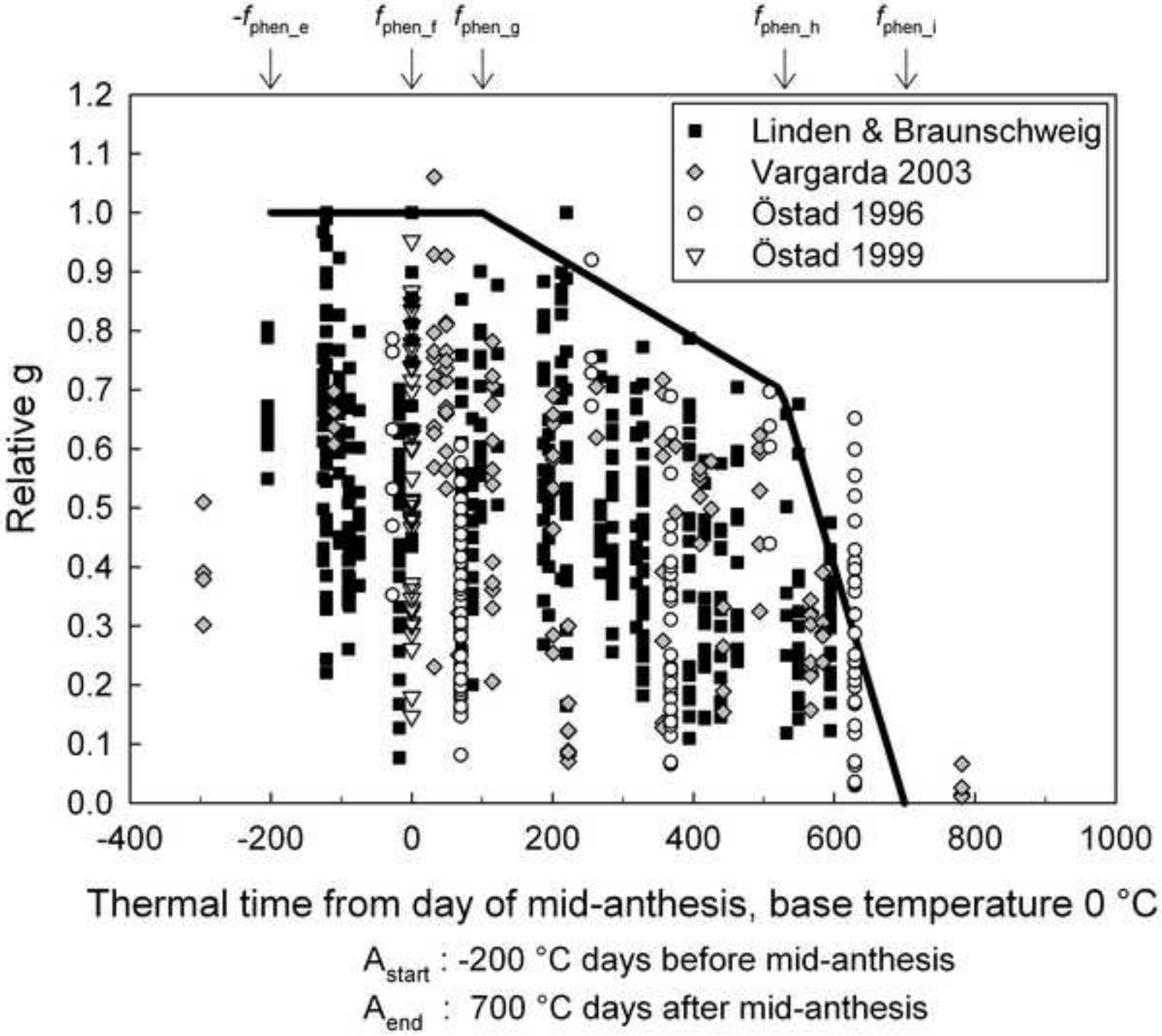

Figure 2b

Click here to download high resolution image

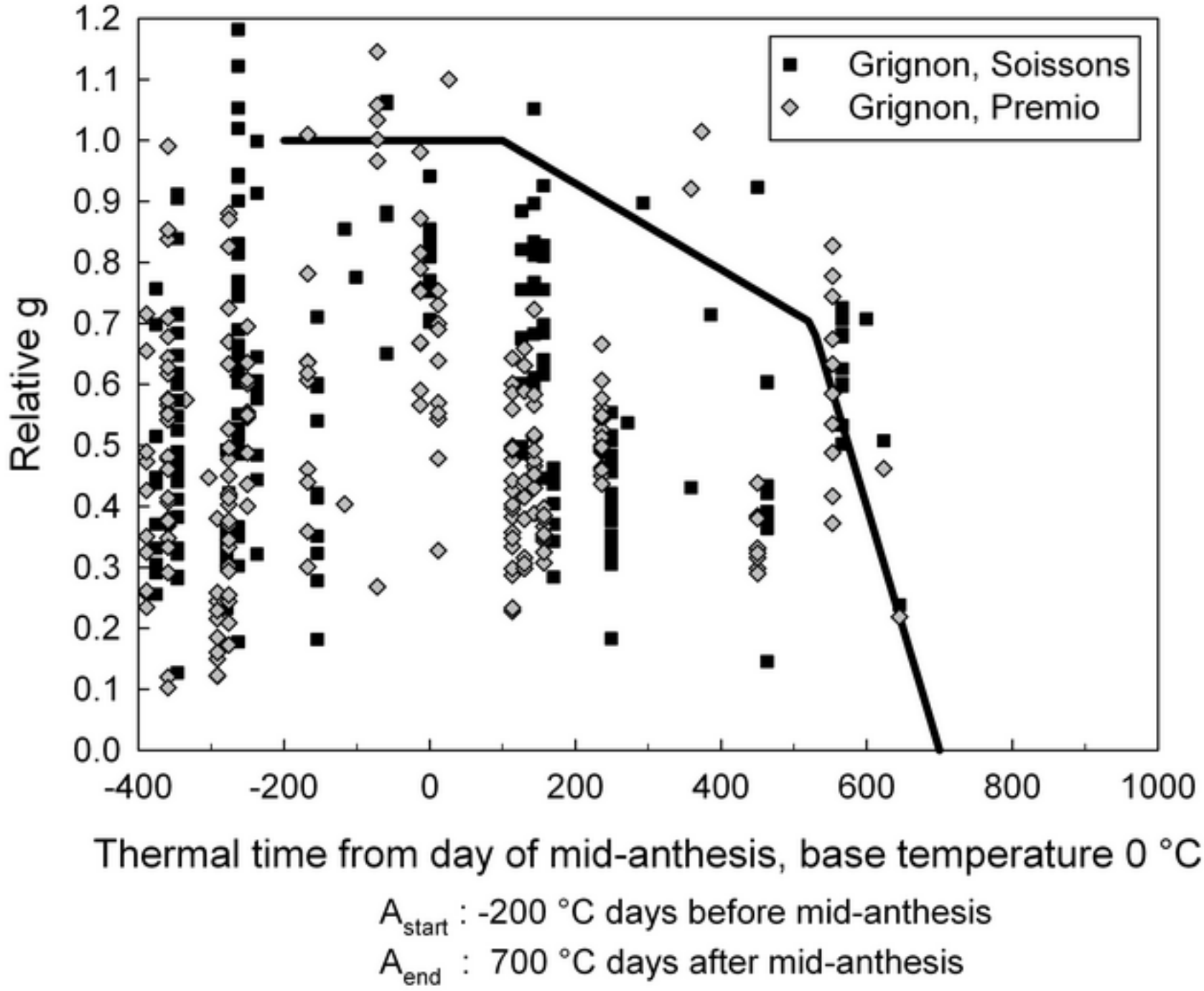

Figure 3

Click here to download high resolution image

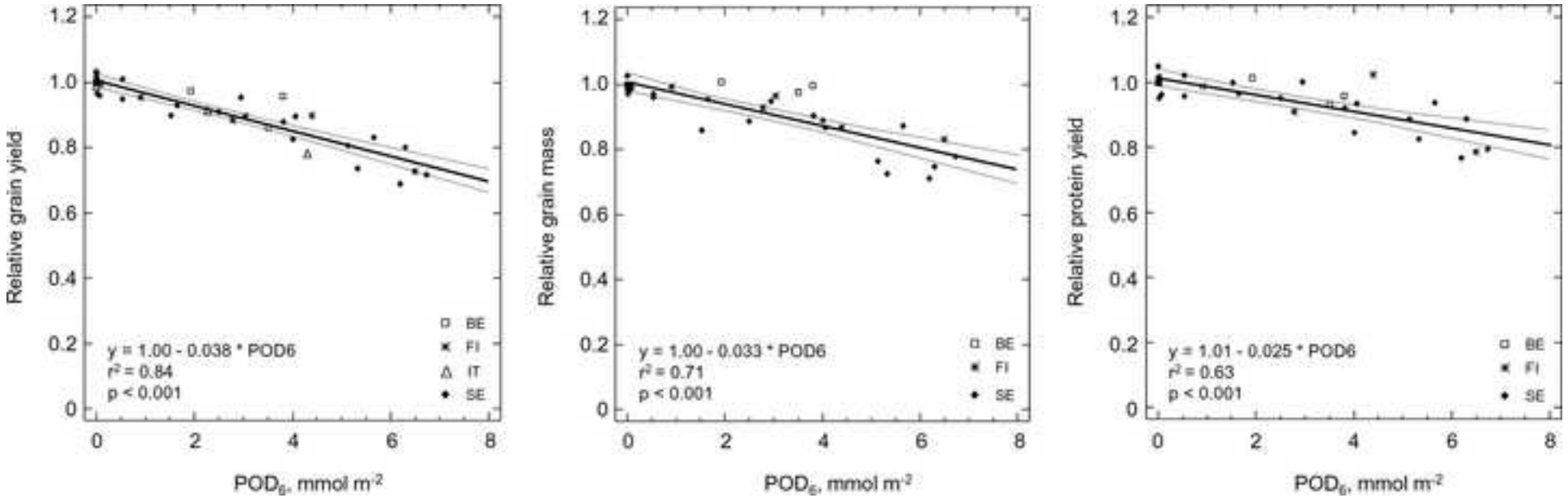

Figure 4

Click here to download high resolution image

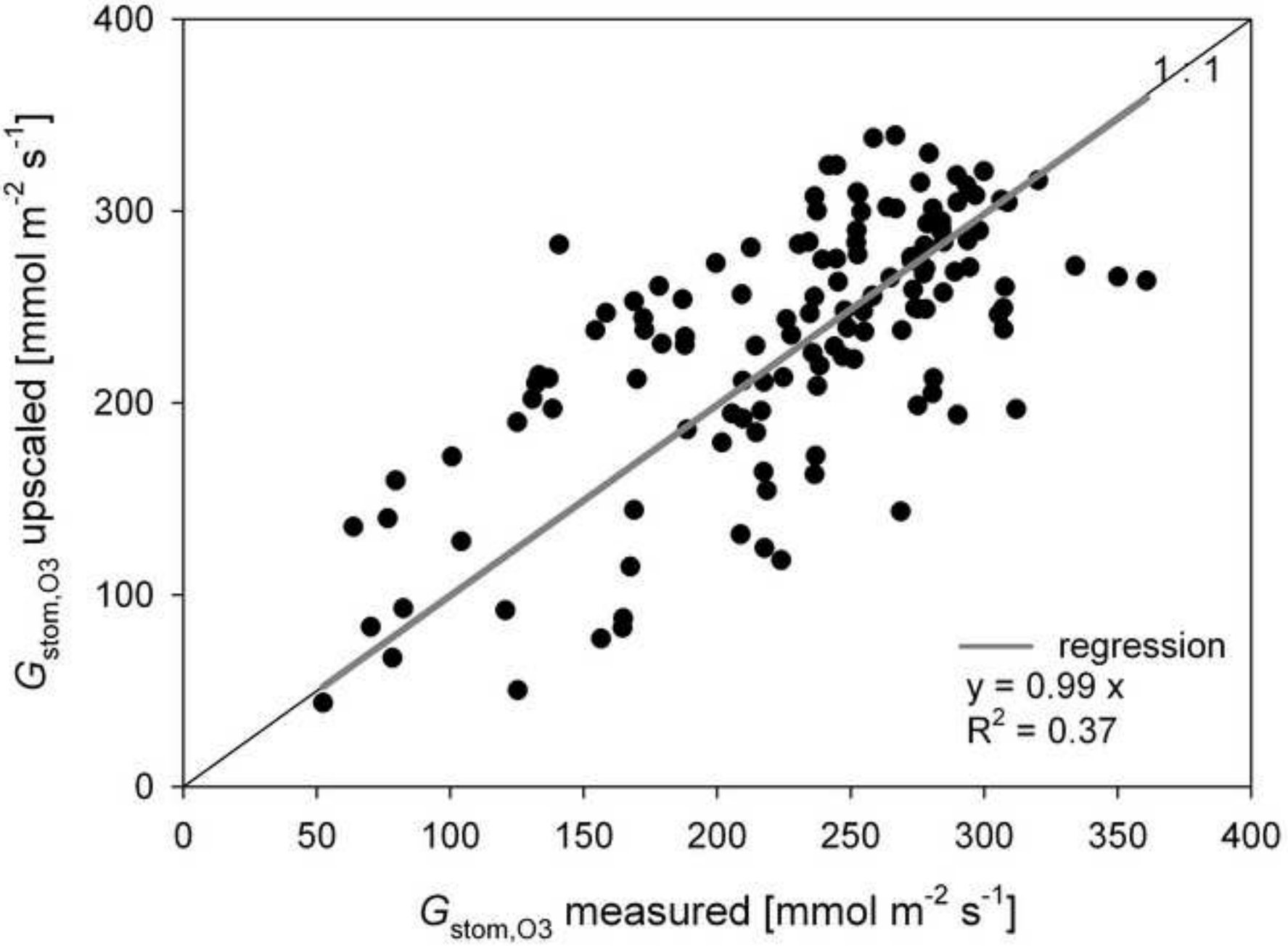

Figure 5 b&w

Click here to download high resolution image

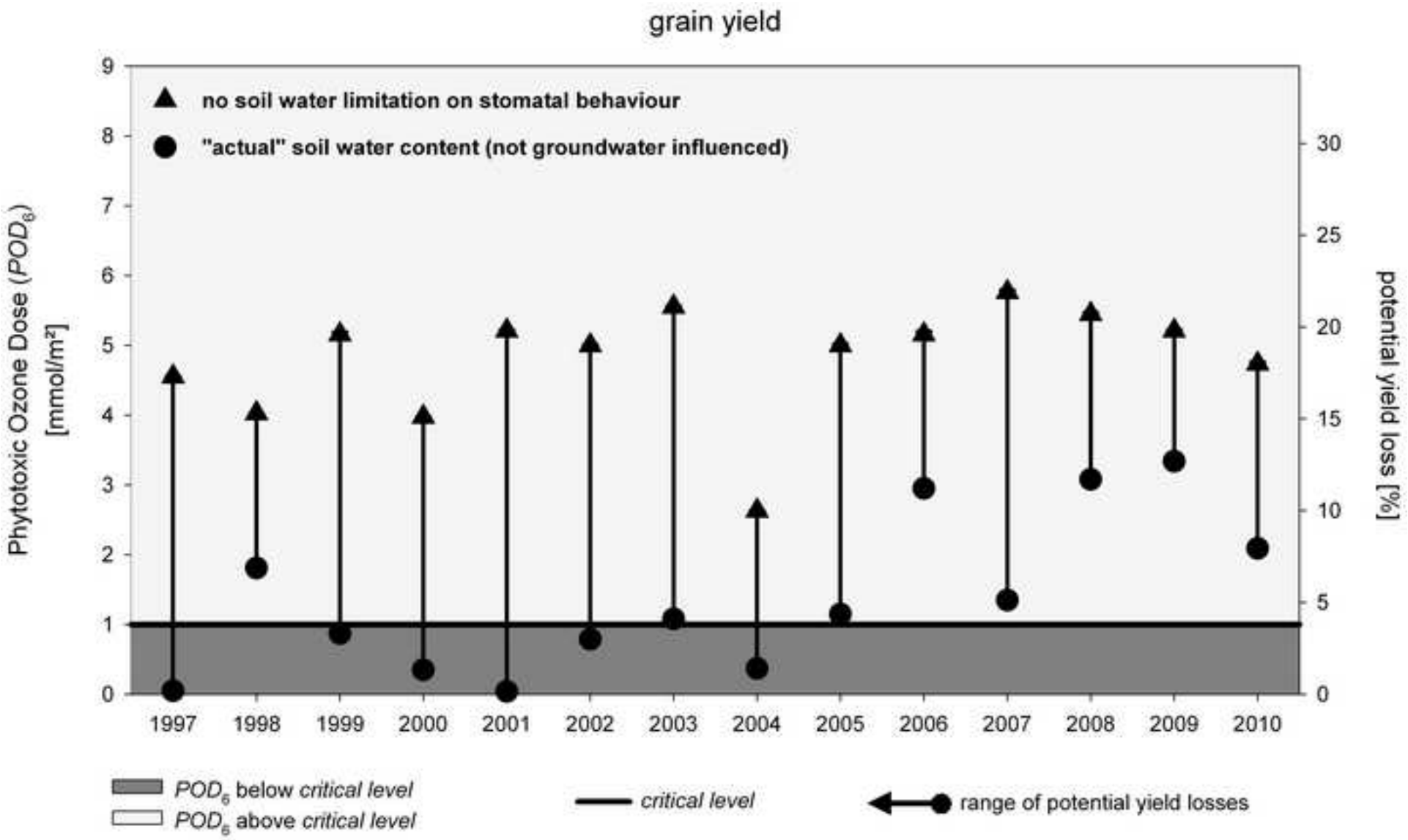

Figure 5 coloured

Click here to download high resolution image

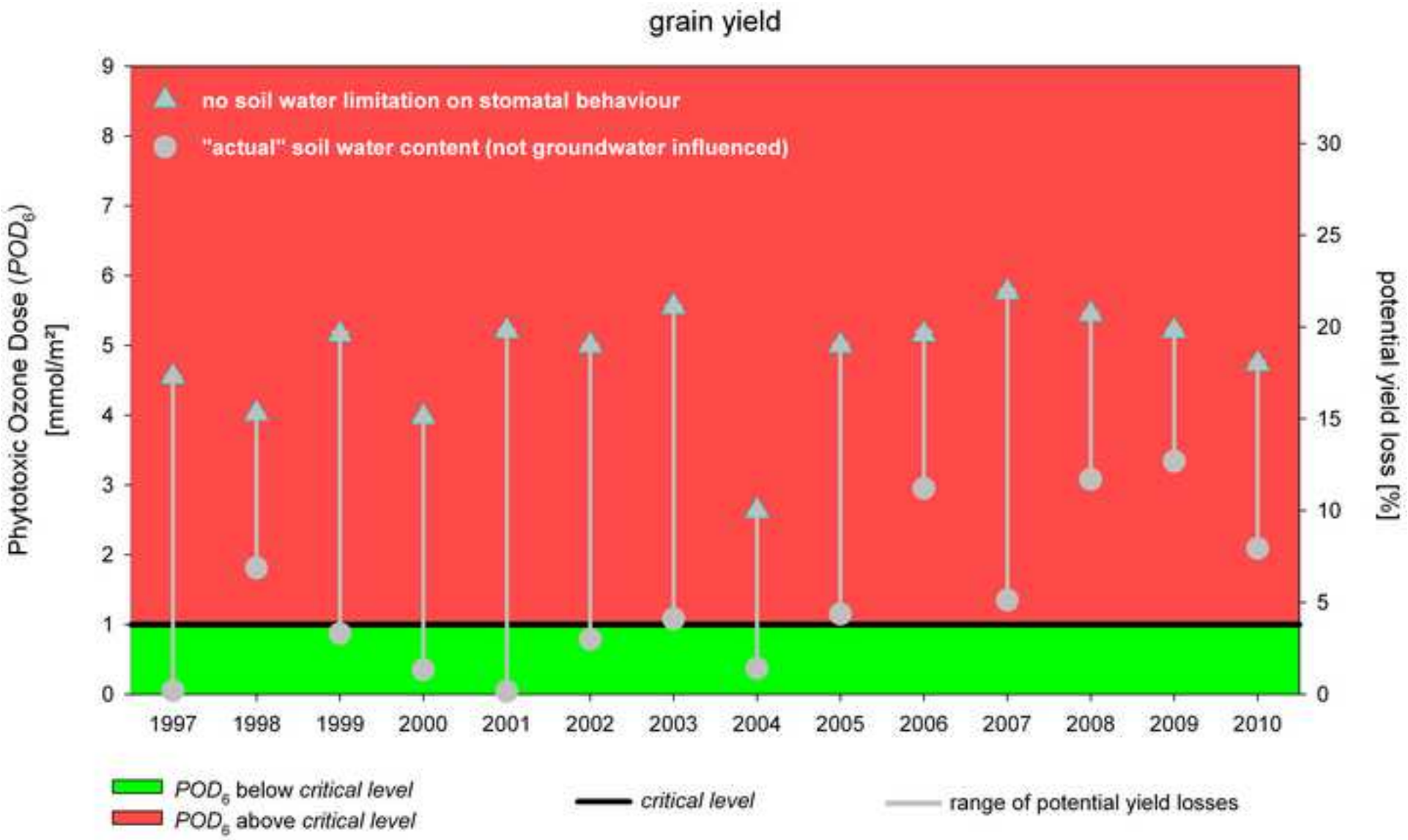

Figure 6a b&w

Click here to download high resolution image

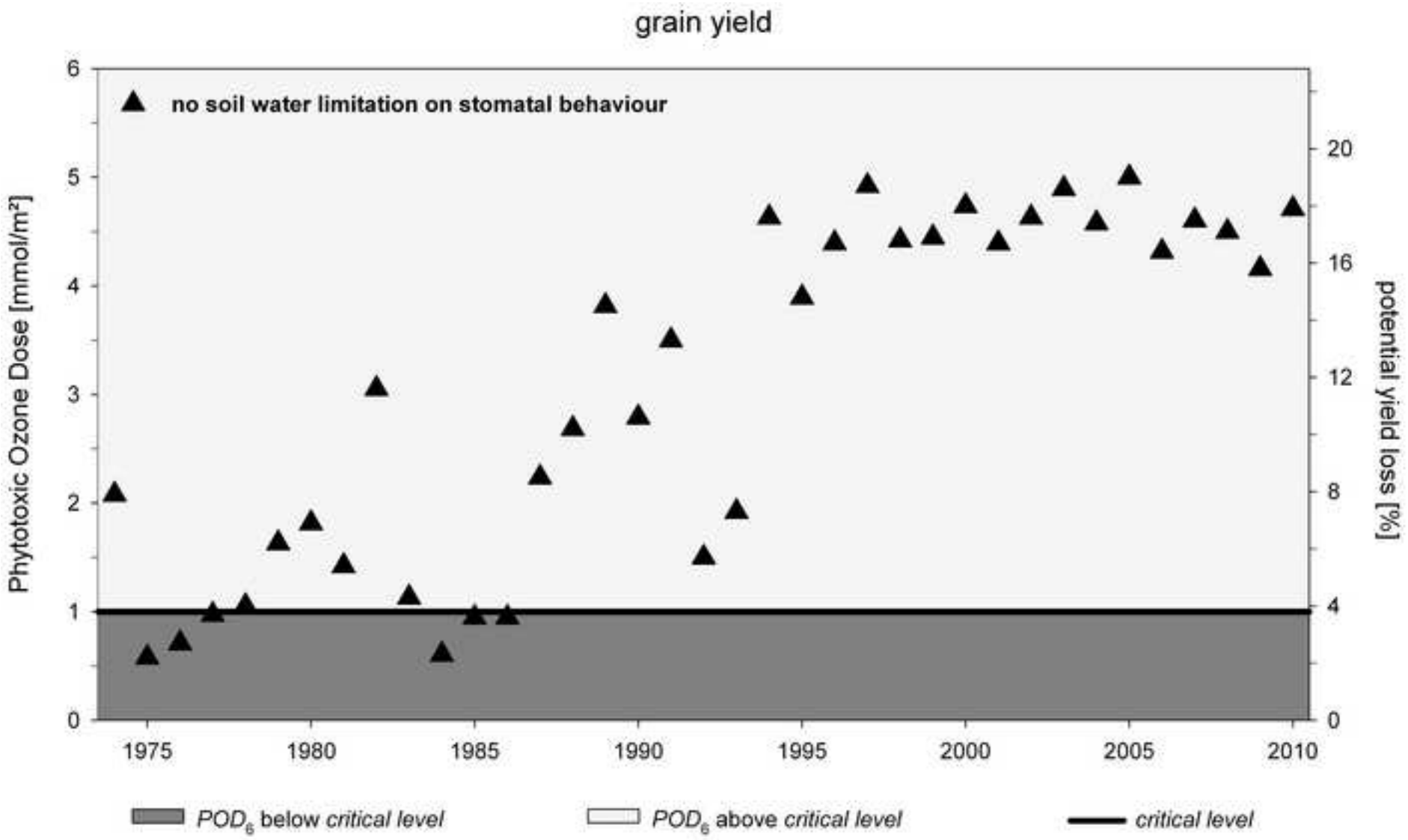

Figure 6a coloured

Click here to download high resolution image

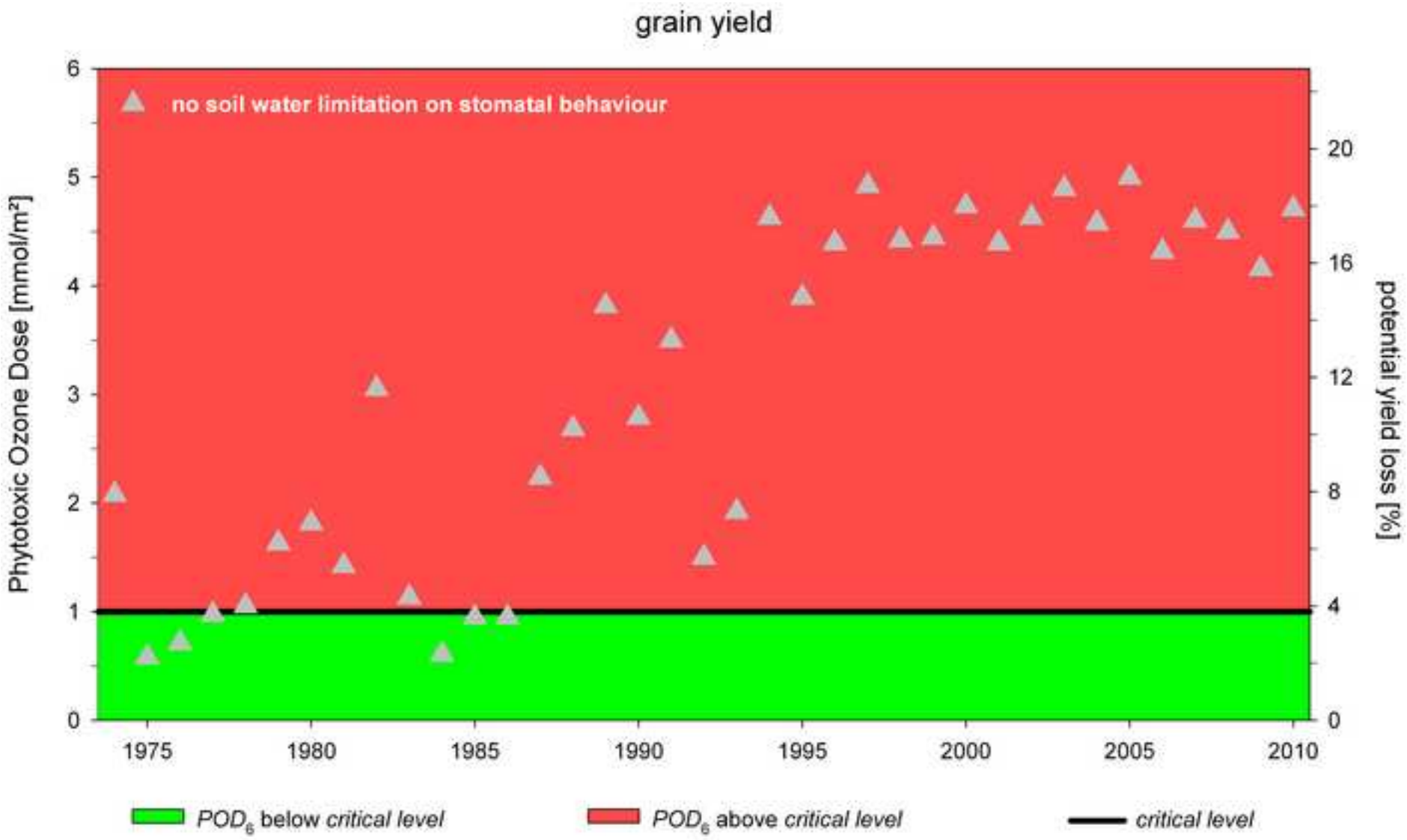

Figure 6b b&w

Click here to download high resolution image

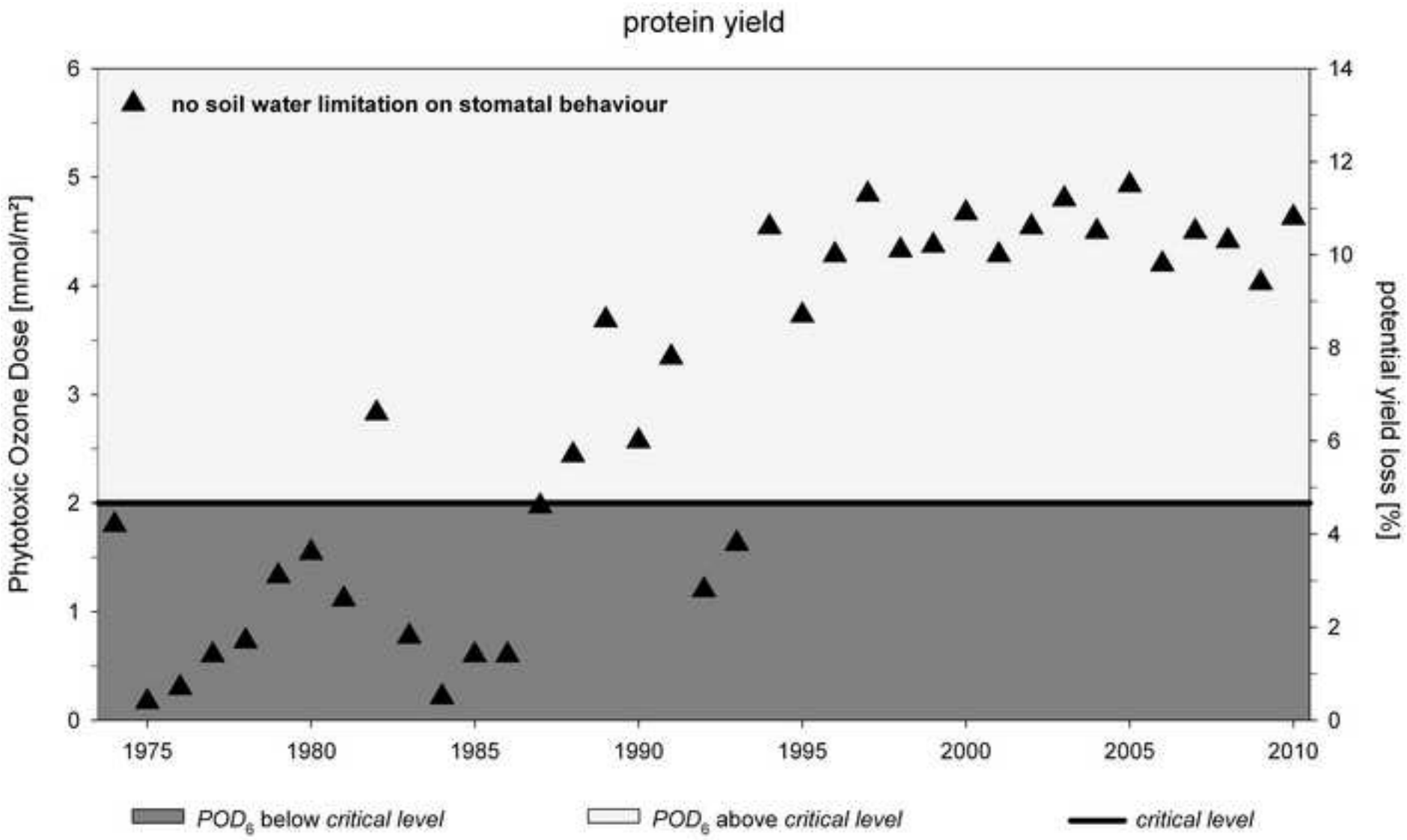

Figure 6b coloured

Click here to download high resolution image

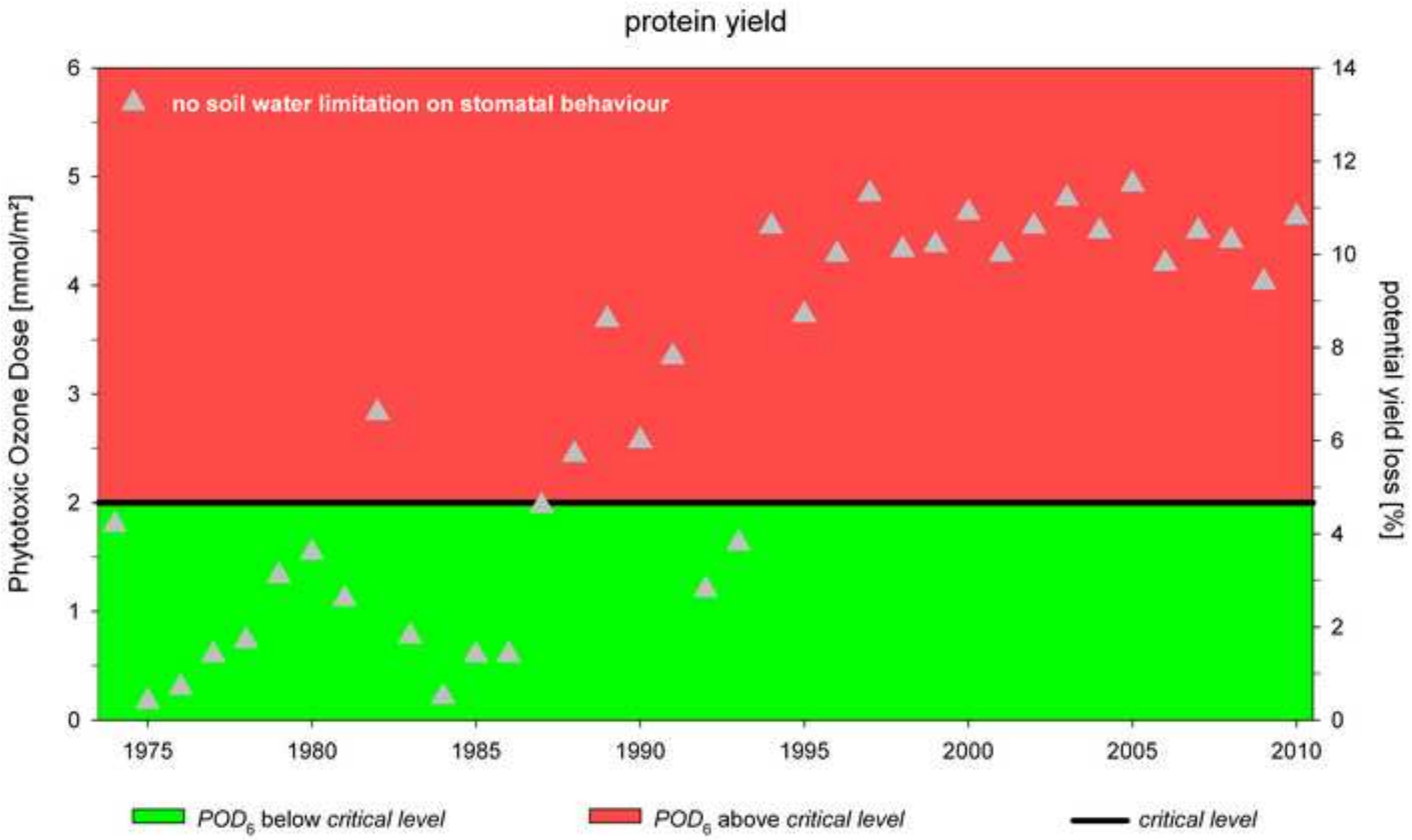

Figure 7 b&w

Click here to download high resolution image

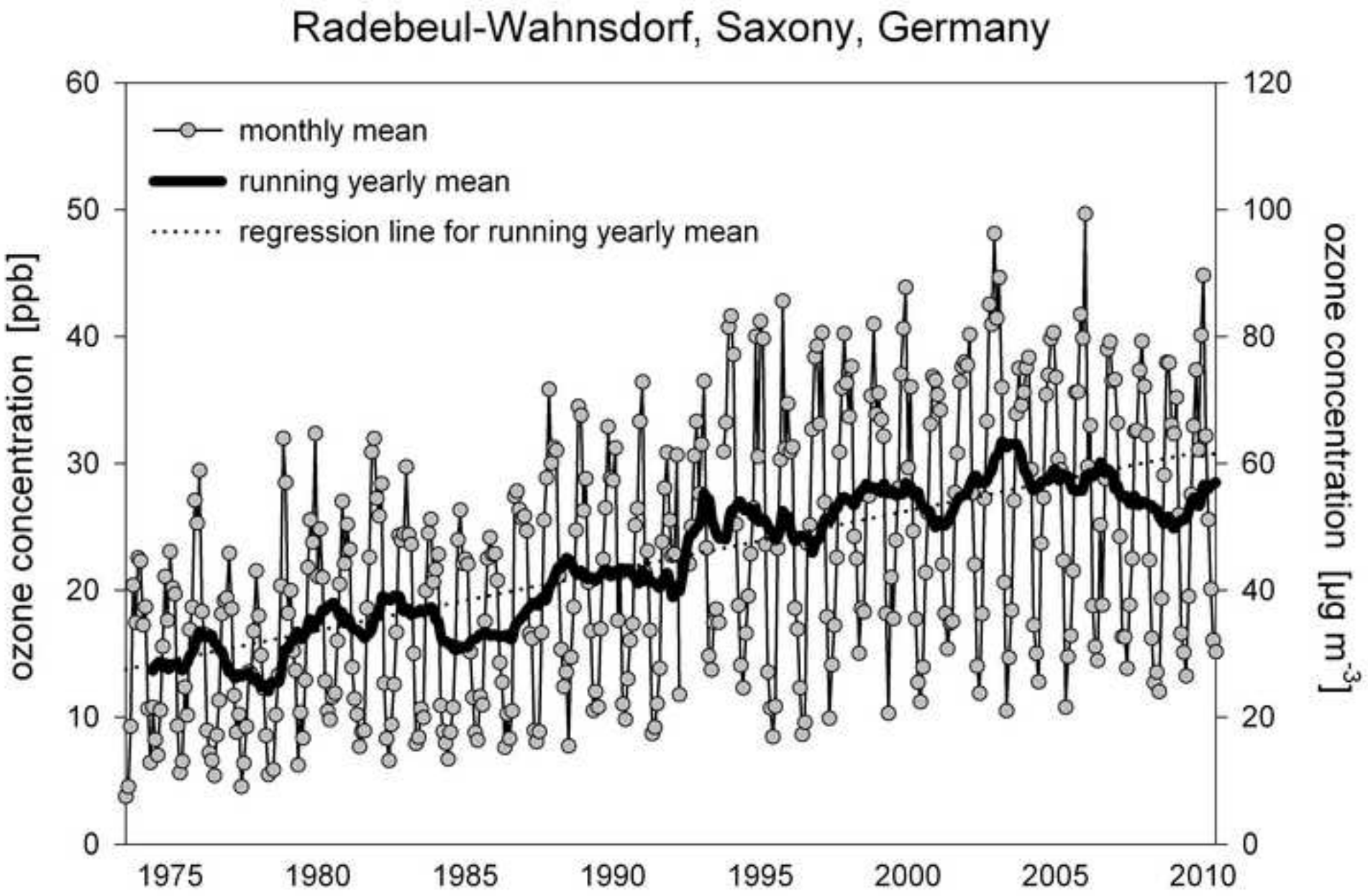

Figure 7 coloured

Click here to download high resolution image